Toward Chain Extension in Crystals of Fluorinated Copolymers As Revealed by Real Time Ultra-Small-Angle X-ray Scattering

E. López Cabarcos and B. de las Rivas

Departamento de Química Física II, Facultad de Farmacia, Universidad Complutense, Madrid 28040, Spain

T. A. Ezquerra and F. J. Baltá Calleja*

Instituto de Estructura de la Materia, CSIC, Serrano 119, Madrid 28006, Spain

Received January 29, 1996; Revised Manuscript Received January 2, 1998

ABSTRACT: We have measured with the ultra-small-angle scattering technique, USAXS, long periods of the order of 120−130 nm in fluorinated copolymers. These unusually large spacings were obtained when copolymers of vinylidene fluoride and trifluoroethylene, with 60% and 80% molar content of vinylidene fluoride, were annealed near the melting point. The formation of crystal stacks during annealing up to a long period of 120 nm was followed in real time. The growth of structures giving rise to long periods of about 100 nm was also observed upon crystallization from the melt. Annealing experiments performed in the hexagonal and in the orthorhombic phases show that polymorphism plays an important role in the thickening of the crystals in accordance with the predictions of the chain sliding diffusion theory.

Introduction

Melt-crystallized synthetic polymers usually exhibit a spherulitic morphology in which "chain folded" lamellae are arranged radially in the polycrystalline aggregate. The appearance of "extended chain" crystals (thichnesses commensurate with molecular length) (ECCs) in polymers is less common and has attracted attention in recent years as it was demonstrated to occur not only at high pressure[1−3] but also at atmospheric pressure.[4−7] Basset and Turner involved in their early work[3] the intervention of a phase, with hexagonal symmetry for crystallization under high pressure. More recently, Hikosaka[8] proposed a chain sliding diffusion mechanism along the chain axis within the hexagonal phase to explain the formation of ECCs. The existence of such an hexagonal phase has been shown to be a requirement for the formation of ECCs.[9]

It is well-known that copolymers of vinylidene fluoride and trifluoroethylene (VF_2/F_3E) exhibit two crystalline phases at atmospheric pressure: an orthorhombic phase and an hexagonal one. The orthorhombic, low-temperature phase presents ferroelectric properties whereas the hexagonal high-temperature phase shows a paraelectric behavior.[10−13] The occurrence of an hexagonal phase in these fluorinated hydrocarbon polymers above the Curie temperature, T_c, identifies them as suitable candidates for the achievement of extended chain morphologies at atmospheric pressure. Thus, thick lamellar single crystals are found to grow in P(VF_2/F_3E) copolymer films when annealed above the Curie temperature.[14] Large bulk crystals with various crystal habits were also found to develop in annealed films.[14] The use of optical and electron microscopy has led to the observation of ECCs morphologies in 72/28, 75/25, and 81/19%mol % VF_2/F_3E copolymers.[14] Ohigashi et al. explained the growth of large single crystals through diffusive displacement of highly mobile molecular chains in the hexagonal phase above T_C. In annealed films, 0.1 μm thick lamellae with 5−10 μm in lateral width were developed. Melt crystallization of PVF_2 at high pressures (above 3 kb) also yields thick extended chain lamellar crystals.[15]

Although the structure of the VF_2/F_3E copolymers has been extensively studied using wide-angle X-ray diffraction, there are still few studies using small-angle X-ray scattering (SAXS) that span a reasonable range of crystallization temperatures.[16−19] In annealing studies performed with copolymers having 54 and 75% VF_2 molar content, the absence of detectable long spacings has been interpreted in the light of various alternatives: to the presence of dilute microvoids, to a nematic liquid crystalline structure, or to the occurrence of thick lamellar crystals with long periods of several hundred nanometers.[20] However, SAXS studies could not show until now scattering phenomena of stacks of thick lamellae due to the lack of instruments with appropriate high resolution. The USAXS beamline at HASYLAB allows one to record SAXS patterns of high resolution in relatively short measuring times, thus offering the possibility to distinguish between the above alternatives.

The aims of this paper are 2-fold.

(1) The first is to follow in isotropic fluorinated copolymers—by means of ultra-small-angle X-ray scattering—the formation during heat treatment, of thick crystal morphologies giving rise to very large spacings. We have selected for this work the 60/40 and 80/20 mol % VF_2/F_3E compositions, as the structure and dynamics of these copolymers are well characterized in our laboratory.[13,21]

(2) The second is to examine the implications of the chain sliding diffusion theory,[8] which predicts that polymers render ECCs if they crystallize or are annealed into the mobile hexagonal phase.

Experimental Section

Materials Preparation. Commercial pellets of poly(VF_2/F_3E), 60/40 and 80/20 mol %, from Atochem were pressure-

S0024-9297(96)00135-0 CCC: $15.00
Published on Web 08/19/1998

Table 1. Curie Temperature and Melting Temperature Values for the Copolymers 60/40 and 80/20 mol % VF_2/F_3E and Molecular Weight of the 60/40 Sample

% VF_2	T_C/K	T_m/K	M_n	M_n/M_w
60/40	340	427	240 000	1.4
80/20	413	423		

molded, at 473 K over 5 min, to 150−250 μm thick films and then quenched in water at 293 K. WAXS patterns show that the samples in the orthorhombic phase are isotropic. Table 1 summarizes the Curie (T_c) and melting temperatures (T_m) for both copolymers. T_c and T_m are average values which may vary depending on sample preparation and thermal history.[13]

Techniques. Experiments were performed in the Ultra-SAXS beamline BW4 at HASYLAB, Hamburg. The USAXS instrument, having pinhole collimation, a double-focusing mirror, and double-crystal monochromator, has been installed at a 38-pole wiggler with a critical energy of 13.6 keV. The distance between the sample and the detector was 12.1 m and the X-ray wavelength 1.3868 Å. The beam path was kept in a vacuum (10^{-6} mbar) and the beam size at the sample was about 1 × 2 mm^2. The range of scattering vectors available at 12.1 m distance covers 4×10^{-4} to 4.2×10^{-3} Å^{-1}. A 200 × 200 mm^2 multiwire proportional counter with delay line and carbon window was used to record the scattering patterns.

During the X-ray scattering experiments, the isotropic films were placed in a temperature chamber. To ensure good and rapid thermal equilibrium within the polymer and homogeneous heating, all samples were wrapped in 0.01 mm aluminum foil. The samples were heated at 1 K/min until the annealing temperature was reached. The time required to register each pattern was 5 min and the annealing times were taken at the end of the recording process. In one experiment the data were collected during the heating scan. In that case the polymer was heated at 1 K/min until the recording temperature, left five minutes at that temperature, while the pattern was collected, and heated again at 1 K/min to the next temperature.

Determination of the Structural Parameters. The USAXS data were used to determine typical structural parameters of semicrystalline polymers.[22] An approximate estimate of the crystal size is made by assuming the sample to consist of a stacking of lamellae showing electron density variations in the direction of stacking. If one considers an isotropic distribution of stacks the one-dimensional (Lorentz corrected) intensity function is given by[22]

$$I(s) = 4\pi I_s s^2 \tag{1}$$

where I_s is the scattering intensity, s is the magnitude of the scattering vector ($s = 2(\sin\theta)/\lambda$), θ is the scattering angle, and λ is the X-ray wavelength. In the stack model the long spacing L can be calculated from the position of the maximum at the Lorentz-corrected SAXS curves

$$L = 1/s \tag{2}$$

L is equal to the sum of crystalline $\langle l_c \rangle$ and amorphous $\langle l_a \rangle$, layer thicknesses, where $\langle l_c \rangle = X_c L$ and $\langle l_a \rangle = (1 - X_c)L$ and X_c is the crystallinity.

In a more elaborate analysis, one can calculate the one-dimensional correlation function[22,23] which is the inverse cosine Fourier transform of the scattered intensity:

$$\gamma(r) = \int_0^\infty I(s) \cos(2\pi s r)\, ds \tag{3}$$

To properly calculate the correlation function, the scattered intensity must be corrected by the liquid scattering intensity, I_b, and interphase corrections must also be considered. Thus, the correlation function reads[24,25]

$$\gamma(r) = \int_0^\infty (I - I_b)s^2 \exp(4\pi^2 s^2 \sigma^2) \cos(2\pi s r)\, ds \tag{4}$$

Here, σ is related to the width of the crystal-liquid interphase E by $E = \sigma(12)^{1/2}$.

For the ideal two-phase model the correlation function allows one to evaluate the long period from the first maximum of $\gamma(r)$, L_c^M. An additional estimate from the long spacing can be obtained from doubling the magnitude of the first minimum, L_c^m. The concentration of both phases can be calculated by[23]

$$x_1 x_2 = R/L_c^M \tag{5}$$

where $x_1 + x_2 = 1$, R is the position of the first intercept of $\gamma(r)$ with the abscissa, and $x_1 = l_1/L_c^M$, l_1 and $l_2 = L - l_1$ being the thickness values of each phase. It is noteworthy that the analysis of the correlation function does not allow to determine which one of the two phases corresponds to the amorphous or the crystalline one. The calculation of the correlation function was done by using the program SASDAP.[24,25]

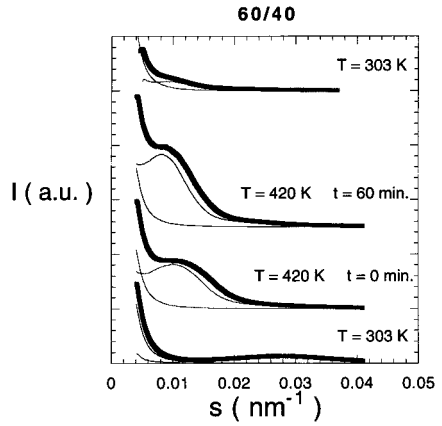

Figure 1. Experimental scattering curves of 60/40 copolymer at different conditions (thick traces). The scattering curves after background correction are also represented (thin traces).

Results

(i) Annealing Behavior. The raw intensity pattern at 303 K shows a well-defined maximum which, after the material is heated to 420 K and annealed at this temperature, shifts to smaller angles. Figure 1 illustrates the scattering curves, before and after background subtraction (without s^2 weighing) showing the development of the SAXS peak during heating (from 303 to 420 K), subsequent annealing (60 min at 420 K) and after cooling at room temperature (from 420 to 303 K). The correlation functions corresponding to the three scattering patterns of Figure 1 are shown in Figure 2. One sees that the position of the different maxima and minima of $\gamma(r)$ depends of thermal treatment. In Table 2 the different structural parameters calculated both from the USAXS patterns (L) and from the analysis of the correlation function (L_c^M, L_c^m, l_1, and l_2) are presented. As shown in Table 2, the thickness of the larger fraction, l_1, increases during the annealing at 420 K from 48 nm at the beginning of the treatment to 56.6 nm after 1 h.

The real-time Lorentz-corrected SAXS curves for the 60/40 copolymer measured during the heating process at temperatures below, through and above the Curie temperature region are shown in Figure 3. The values of the long period calculated using eq 2 are shown in

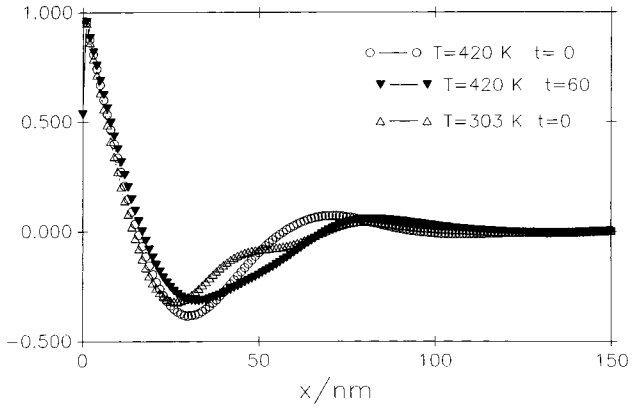

Figure 2. Linear correlation functions $\gamma(r)$ corresponding to the scattering patterns of Figure 1.

Table 2. Experimental Values for the Bragg Long Period, L, together with the L_c^M, L_c^m, l_1, l_2, and Linear Crystallinity, X_{cL}, Values Obtained from the Analysis of the Correlation Function and Number of Folds per Crystal, for the 60/40 Copolymer Annealed under Various Conditions

T/K	t/min	L/nm	L_c^M/nm	L_c^m/nm	l_1/nm	l_2/nm	X_{CL}	n
420	0	73.8	72	62	48	24	0.67	20
420	60	91.4	83	66	56.6	26.4	0.68	18.3
303	0	80.5	81	54	61	19	0.75	17

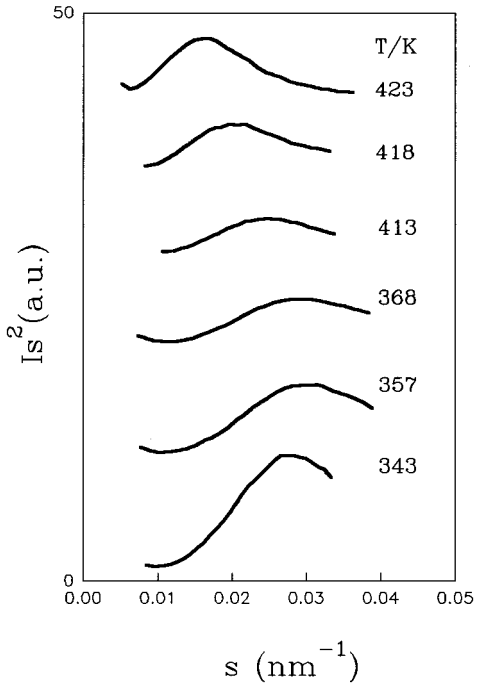

Figure 3. Small-angle X-ray scattering patterns at the indicated temperatures, obtained during heating of the 60/40 VF_2/F_3E copolymer. The magnitude of the scattering vector is defined by $s = (2\pi/\lambda)(\sin\theta)$ (see text).

Figure 4. Here one sees that at the onset of the ferro-paraelectric transition there is a stepwise decrease in L.[21] After the ferro-to-paraelectric transition (340 K) is completed, at T_c, L increases further with increasing temperature as is known to occur in other polymers.

To follow the kinetics of the long period growth in the 60/40 copolymer we have carried out USAXS experiments on three samples with different starting L values using three different annealing temperatures (423, 420, and 398 K). Figure 5a illustrates the gradual shift of the SAXS maximum toward smaller scattering angles

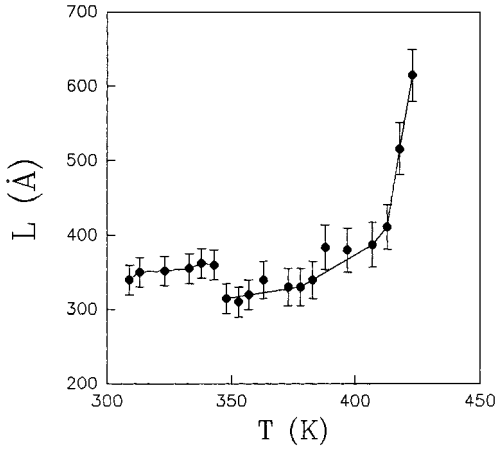

Figure 4. Temperature dependence of the long period for the 60/40 copolymer.

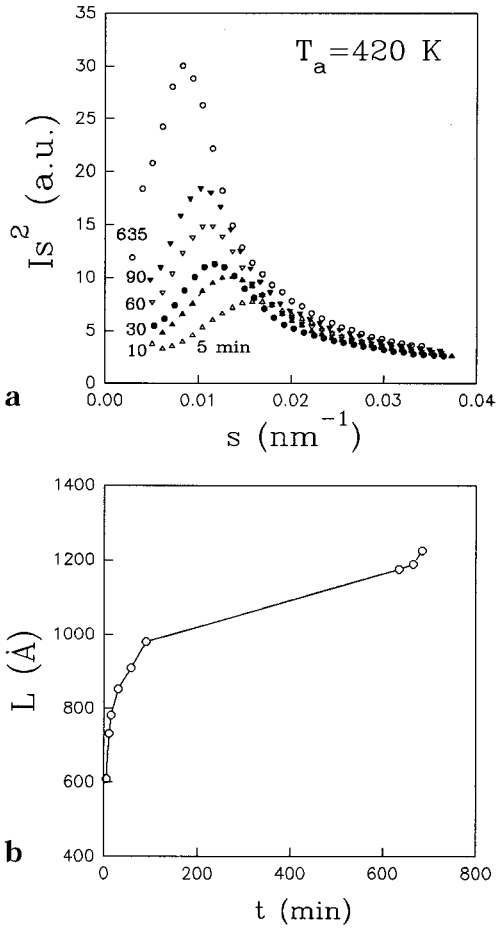

Figure 5. SAXS patterns for the 60/40 copolymer at 420 K: (a) changes in the scattering profile as a function of annealing; (b) plot of L as a function of t at 420 K.

as a function of the annealing time for the sample annealed at 420 ± 1 K. An increase of scattering intensity and a concurrent narrowing of the scattering maximum is observed. Figure 5b shows a continuous increase of L with t reaching after t = 635 min of annealing values higher than 1200 Å (Figure 5b). To our knowledge this is the first time that such large long spacings have been reported in these copolymers using X-ray scattering techniques. Figure 6 illustrates the time-resolved wide-angle X-ray diffraction (WAXS) profiles during the annealing process at 420 K. As can be seen, no appreciable change in the WAXS profiles in the

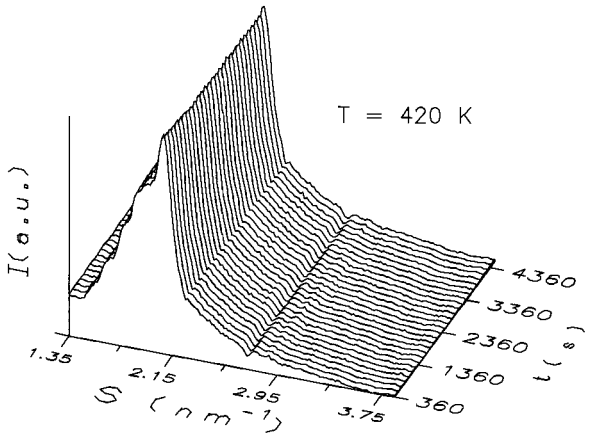

Figure 6. Time-resolved WAXS profiles of the 60/40 copolymer during annealing at 420 K. The profiles shown as a function of annealing time, are equally increased in time with the full range of this experiment being 4360 s.

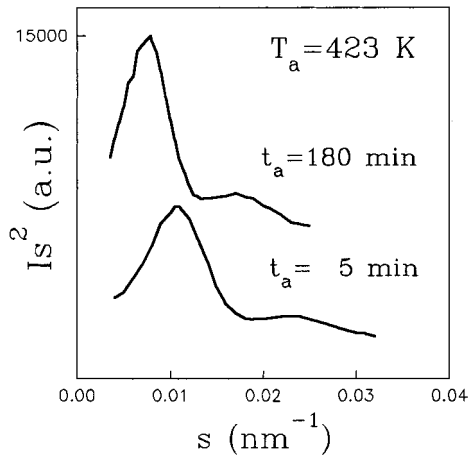

Figure 7. SAXS patterns for the 60/40 copolymer annealed at 423 K for various t_a values.

range of annealing times investigated is detected. Thus, during annealing, while the long spacing increases (Figure 5b), the crystallinity remains constant.

Annealing at a higher annealing temperature (423 ± 1 K) results in scattering patterns showing two maxima (see Figure 7). Already, after 5 min of annealing time at $T_A = 423$ K, the scattering curve shows two spacings at, $L_1 \approx 97$ nm and $L_2 \approx 46$ nm. These long periods further increase up to $L_1 \approx 137$ nm and $L_2 \approx 59$ nm after annealing for 180 min. The simultaneous shift of both peaks and the fact that the larger spacing is close to twice the value of the smaller suggest that we are dealing with two orders of the same periodicity.

(ii) Influence of the Hexagonal Phase on the Kinetics of Annealing. As mentioned above the occurrence of an hexagonal phase is a prerequisite to obtain a molecular extended chain conformation in polymers. To find out whether the occurrence of the hexagonal phase is also crucial in case of fluorinated copolymers, we have performed the following experiment: two samples were annealed in the hexagonal phase and in the orthorhombic phase, respectively, in such a way that the value $\Delta T = T_m - T_a$ is equal for both systems while only the symmetry of the crystal phase is different. For this purpose we have used the 80/20 and 60/40 copolymers in which, at $\Delta T = 25$ K, the orthorhombic and hexagonal phase appear, respectively. Thus we, independently, can compare the influence of the crystal phase on the annealing behavior of each copolymer. Parts a and b of Figure 8 illustrate the typical scattering profiles of these two polymers at $\Delta T = 25$ K for various annealing times. In the 80/20 copolymer no changes in the USAXS pattern after long annealing times are observed. However, in the 60/40 system, with increasing t_a, one sees a shift of the scattering maximum to smaller scattering angles, although the WAXS pattern does not show any appreciable change (see Figure 9). While the plot of L as a function of t_a (see Figure 10) shows a clear increase tendency for the 60/40 copolymer, in the case of the 80/20 copolymer the L value remains constant in the range of annealing times investigated. At this point is worth noting that samples with different VF_2/F_3E composition but with similar thermal histories show widely differing long periods before annealing.

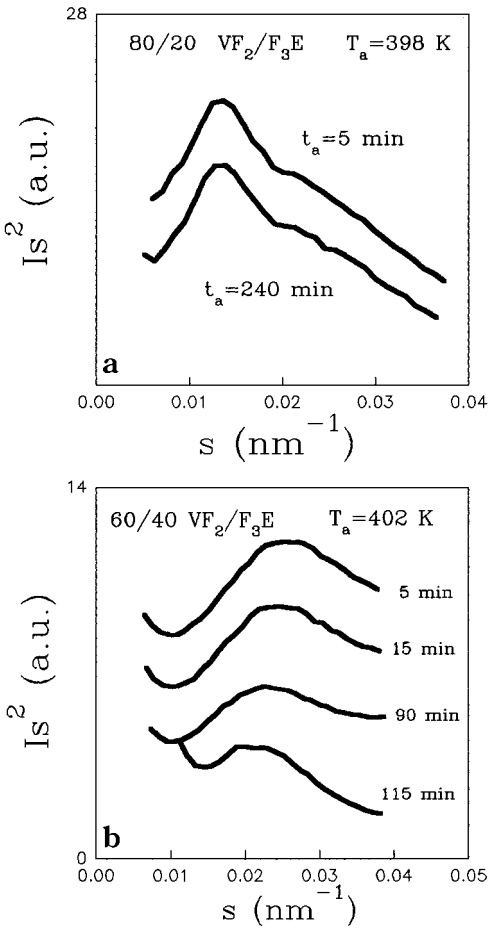

Figure 8. SAXS patterns for (a) the 80/20 copolymer annealed at 398 K (25 K below the melting point), in the orthorhombic phase, at various t_a, and (b) the 60/40 copolymer annealed at 402 K (25 K below the melting point), in the hexagonal phase.

(iii) Crystallization from the Melt. In an attempt to obtain a structure with a large long period at room temperature, a sample of the 60/40 copolymer was crystallized from the melt in the hexagonal phase. After leaving the copolymer in the melt, at 453 K, for 5 min the sample was finally quenched to 413 K. In this case, a shoulder appears after the first 5 min of crystallization at this temperature (see Figure 11). After 2 h at this temperature, the peak increases further in intensity indicating a slow crystallization kinetics at this temperature. The USAXS pattern of Figure 11 exhibits only one maximum corresponding to a long spacing of around 100 nm without any indication of the presence

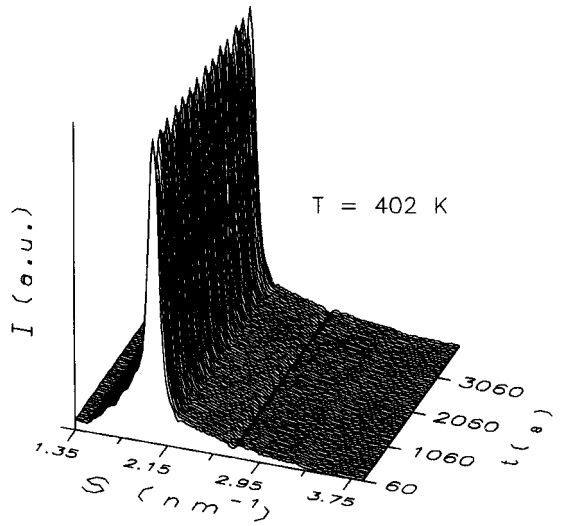

Figure 9. Time-resolved WAXS profiles of the 60/40 copolymer during annealing at 402 K. The profiles, shown as a function of annealing time, are equally increased in time.

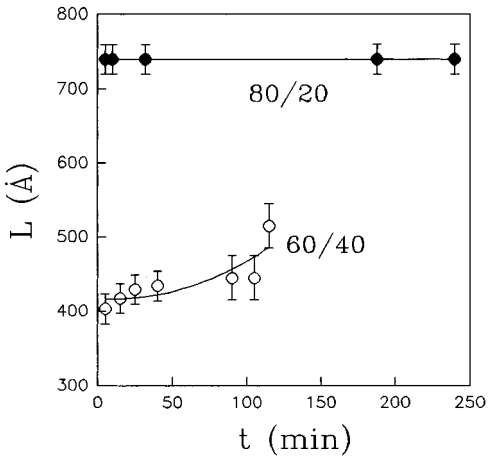

Figure 10. Variation of L as a function of the annealing time for the 60/40 and 80/20 copolymers annealed 25 K below the melting point.

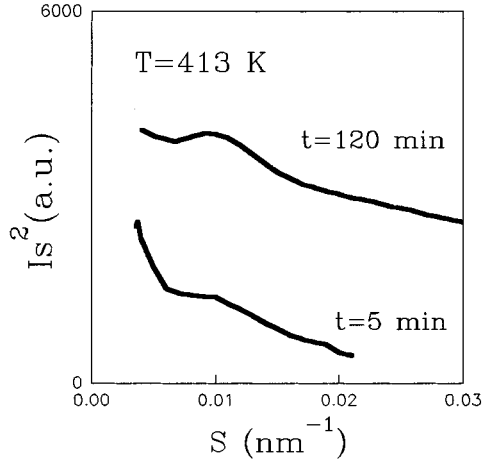

Figure 11. SAXS profiles for the 60/40 copolymer crystallized at 413 K at the times indicated in the figure.

of the second weak reflection. The DSC curve of this sample, performed starting at the crystallization temperature (413 K), shows only one melting peak at 430 K and confirms the growth of only one lamellar size distribution.

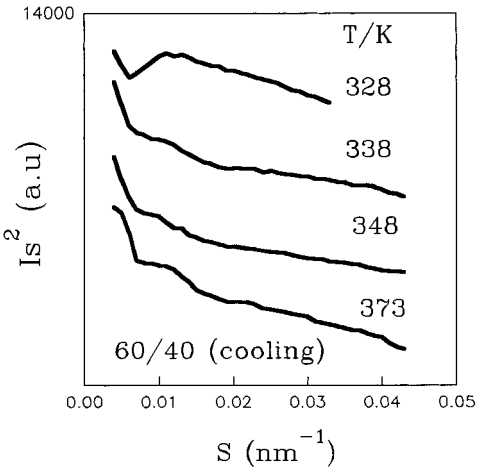

Figure 12. SAXS patterns taken at the indicated temperatures obtained during the cooling process of the copolymer 60/40 crystallized at 413 K (see Figure 13).

During the cooling process to room temperature the maximum at 100 nm decreases its intensity and loses its definition. Below the Curie transition one observes a small L decrease to values near 85 nm accompanied by a considerable broadening as shown in Figure 12. When the sample is cooled below T_c, the initial packing of the thick lamellae grown in the paraelectric phase seems to be distorted, contributing to the broadening of the USAXS peak (Figure 12).

Discussion

Structural Parameters. In previous studies the usual long period dependence with temperature found in different polymers led sometimes to the disappearance of the scattering maximum which may be shifted behind the beam stop at high temperature.[20] Our own investigations indicate that, in case of the 60/40 copolymer, the SAXS long period may vary, depending upon heating and cooling, between 30 and 45 nm.[21] Only recently, after using transmission electron microscopy, was attention drawn to the possibility of extended chain single crystals formation on copolymers with 75/25 and 78/22 compositions.[4]

The results reported in the present study indicate that relatively large L values are observed after annealing the samples near their melting point or by crystallization at 413 K in the hexagonal phase. In addition, once a structure exhibiting a very high periodicity is formed, it can be transferred at room temperature by means of rapid cooling of the sample. Although some distortions may be introduced in the crystal packing when crossing the Curie temperature, the broad maxima centered at 85 nm suggest that part of the stacking structure showing the high periodicity is preserved.

Similarly to other melt crystallized polymers[27,28] our data (Figure 13) show the log annealing time dependence

$$L = B \log t + L_0$$

where the slope of the plot of B depends on the annealing temperature. The value, obtained for T_A = 420 K is B = 272 and for T_A = 402 K is B = 53. It is noteworthy that these B values are considerable larger than those found in other polymers (between 10 and 50 in PE[27] and around 10 in PP[28]). This finding suggests an enhanced contribution to the molecular diffusion

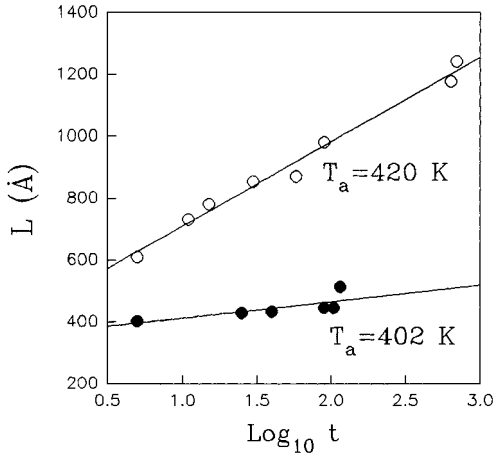

Figure 13. Plot of L vs log t_a for the 60/40 copolymer annealed at 402 and 420 K, respectively.

mechanism present in the hexagonal phase of these copolymers.

Let us next discuss the analysis of structural parameters from the correlation function. First of all, it is necessary to assign to which l value the crystalline phase corresponds and to which one the amorphous phase corresponds. After heat treatment at $T = 420$ K for 60 min and subsequent cooling of the sample at 303 K (room temperature) (Figure 1) one obtains the values $l_1 = 61$ nm and $l_2 = 19.8$ nm. These values of l_1 and l_2 would give a linear degree of crystallinity $X_{cl} = 0.75$, and $l_1 = l_c$ and $l_2 = l_a$ are taken as the thicknesses corresponding to the crystalline and amorphous phases, respectively. This crystallinity value seems reasonable when compared with the degree of crystallinity ($X_c = 0.72$)[21] of this copolymer previously estimated by WAXS measurements.

Moreover, inspection of Table 2 shows that in all cases $L > L_c^M > L_c^m$. This is characteristic of an inhomogeneous distribution of lamellar stacks separated by additional pockets of amorphous material existing between the adjacent stacks of crystalline and amorphous layers.[25]

One comment has to be made in relation to the correlation function $\gamma(r)$ obtained at $T = 303$ K showing an inflection point around 50 nm (Figure 2). This could be interpreted as due to the existence of a second characteristic long spacing which probably originated as a consequence of the crystallization, upon cooling, of the material which was in the molten state at 420 K.

Toward Chain Extended Structures. Under the assumption of the above assignment for l_1 and l_2 values, from the data of Table 2, one observes that isothermal annealing at 420 K for 60 min leads to a slight thickening of the crystals from 48 up to 56.6 nm. Gel permeation chromatography (GPC) of the 60/40 copolymer gives a M_w value of $M_w = 336\,000$ with $M_w/M_n = 1.4$. This M_w value corresponds to an extended chain length of about $l_{ext} = 1040$ nm (assuming an average projection length of the repeating unit of 0.44 nm). Hence, from the crystal thickness data (see Table 2) it turns out that, depending on the treatment conditions, the number of chain folds $n - l_{ext}/l_c$ in the crystals is on the order of 17−20. After 650 min, at $T_a = 420$ K, long periods of about 120 nm are obtained (see Figure 10). If a parallel increase of l_c with L takes place, l_c values of −100 nm are expected, which would imply a number of about 10 folds. Although the crystal thickness at these long annealing times is not large enough to give a chain extended crystal, a considerable extension of the chain molecules is, nevertheless, achieved.

Chain Sliding Difussion. As stated above, for temperatures higher than 410 K, the long period increase parallels a crystallinity decrease. This means that the mechanism of large long-period formation of "chain extended" structures could be driven for the tendency of thinner crystals to melt contributing to the thickening of larger ones.[26] This is not the case for the copolymer annealed at 402 K, i.e., at 25 K below the melting point. Although the hexagonal phase is a kind of nematic liquid crystal, the specific volume change at T_m ($\Delta V/V = 0.058$) is larger than that at T_c ($\Delta V/V = 0.048$) and the latent heat at T_m is double as compared to that at T_c,[13] indicating that interchain interaction remains in the hexagonal phase. However at the orthorhombic−hexagonal phase transition temperature, T_c, the d_{110} spacing of the crystal unit cell and, therefore, the intermolecular lateral distances increases by about 10%.[11,12,17−19] In the hexagonal phase the sliding of chains within the crystals may be much easier because this d_{110} spacing increases abruptly. According to Hikosaka the energy needed to pull up the chain from the crystal is given by the work required to overcome the potential energy. This energy is proportional to its friction constant κ and to the thickness l and can be written as

$$\Delta E = \kappa l > kT$$

Therefore, ΔE becomes larger with crystal thickening. However in the hexagonal phase $\Delta E \ll kT$[8] and does not depend on the thickness l_c. Thus, crystals can grow under local equilibrium conditions, and the chain extension process is feasible tending, as a result, to a ECCs texture.

Studies performed with nuclear magnetic resonance and incoherent neutron scattering have demonstrated the dynamical character of the paraelectric phase.[29] It seems that a molecular chain in the hexagonal phase may slide along the chain direction through translational jump diffusion motion whereas this motion is not activated in the orthorhombic phase, and consequently the process would be inhibited in the latter phase.

In conclusion, ultra-small-angle X-ray scattering has been shown to be capable to follow the crystal thickening process in fluorinated polymers at atmospheric pressure. Evidence for the existence of long periods larger than 100 nm is provided. We have demonstrated that crystal thickening is enhanced in the hexagonal phase in relation to phases of lower mobility, like the orthorhombic one. Finally the usual logarithmic dependence of the long spacing on the annealing time is also confirmed for these fluorinated polymers.

Acknowledgment. Grateful acknowledgments are due to DGICYT (Grants Nos. PB94-0049 and PB95-0397) and to CICYT (Grant No. MAT 97-1811E) for the generous support of this investigation. We thank Drs. M. Bark, R. Gerkhe, U. Lode, and J. Cronauer and Ms. S. Cunis for the generous help with the USAXS beamline and Prof. J. de Abajo and J. M. García for GPC measurements. We thank Prof. B. Hsiao for the SASDAP program and A. Nogales for her calculation of the correlation function.

References and Notes

(1) Bunn, C. W.; Cobbold, A. J.; Palmer, R. P. *J. Polym. Sci.* **1958**, *28*, 365.
(2) Wunderlich, B.; Arakawa, T. *J. Polym. Sci.* **1964**, *A2*, 3697.
(3) Basset, D.C.; Turner, B. *Nature* **1972**, *240*, 146.
(4) Hikosaka, M.; Sakurai, K.; Ohigashi, H.; Koizumi, T. *Jpn. J. Appl. Phys.* **1993**, *32*, 2029.
(5) Rastogi, S.; Ungar, G. *Macromolecules* **1992**, *25*, 1445.
(6) Hikosaka, M.; Sakurai, K.; Ohigashi, H.; Koizumi, T. *Jpn. J. Appl. Phys.* **1993**, *32*, 2780.
(7) Rastogi, S.; Hikosaka, M.; Kawataba, H.; Keller, A. *Macromolecules* **1991**, *24*, 6384.
(8) Hikosaka, M. *Polymer* **1987**, *28*, 1257; Polymer **1990**, *31*, 458.
(9) Bassett, D. C.; Blark, S.; Piermarini, G. J. *J. Appl. Phys.* **1974**, *45*, 4146.
(10) Furukawa, T.; Johnson, G. E.; Bair, E.; Tajitsu, Y.; Chiba, A.; Fukada, E. *Ferroelectrics* **1981**, *32*, 61.
(11) Lovinger, A. J. *Science* **1983**, *220*, 1115.
(12) Tashiro, K.; Takano, K.; Kobayashi, M.; Chatani, Y.; Tadokoro, H. *Ferroelectrics* **1984**, *57*, 297.
(13) Balta Calleja, F. J.; Gonzalez Arche, A.; Ezquerra, T. A.; Santa Cruz, C.; Batallan, F.; Frick, B.; Lopez Cabarcos, E. *Adv. Polym. Sci.* **1993**, *108*, 1.
(14) Ohigashi, H.; Akama, S.; Koga, K. *Jpn. J. Appl. Phys.* **1988**, *27*, 2144.
(15) Matsushige, K.; Takemura, T. *J. Cryst. Growth* **1980**, *48*, 343.
(16) Lovinger, A. J.; Davis, G. T.; Furukawa, T.; Broadhurst, M. G. *Macromolecules* **1982**, *15*, 323.
(17) Davis, G. T.; Furukawa, T.; Lovinger, A. J.; Broadhurst, M. G. *Macromolecules* **1982**, *15*, 329.
(18) Lovinger, A. J.; Furukawa, T.; Davis, G. T.; Broadhurst, M. G. *Polymer* **1983**, *24*, 1225; *Polymer* **1983**, *24*, 1233.
(19) Tashiro, K.; Takano, K.; Kobayashi, M.; Chatani, Y.; Tadokoro, H. *Polymer* **1981**, *22*, 1312; *Polymer* **1984**, *25*, 195.
(20) Victoria Fernandez, M.; Suzuki, A.; Chiba, A. *Macromolecules* **1987**, *20*, 1806.
(21) Lopez Cabarcos, E.; Gonzalez Arche, A.; Balta Calleja, F. J.; Bösecke, P.; Röber, S.; Bark, M.; Zachmann, H. G. *Polymer* **1991**, *32*, 3097.
(22) Baltá-Calleja, F. J., Vonk, C. *X-ray Scattering of Synthetic Polymers*; *Elsevier Sci. Publishers*: New York, 1989; p 249.
(23) Strobl, G.; Schneider, M. J. *J. Polym. Sci., Part B: Polym. Phys.* **1981**, *8*, 1355.
(24) Verma, R.; Biswas, A.; Hsiao, B. S.; Marand, H. *J. Appl. Crystallogr.*, in Press.
(25) Verma, R.; Marand, H.; Hsiao, B. S. *Macromolecules* **1996**, *29*, 7767.
(26) Yeh, G. S. Y.; Hosemann, R.; Loboda-Cackovic, J.; Cackovic, H. *Polymer* **1976**, *17*, 309.
(27) Fischer, E. W.; Schmidt, G. F. *Angew. Chem. Int Ed. Engl.* **1962**, *1*, 488.
(28) Balta Calleja, F. J.; Peterlin, A. *Makromol. Chem.* **1971**, *141*, 91.
(29) Lopez Cabarcos, E.; Batallan, F.; Frick, B.; Ezquerra, T. A.; Balta Calleja, F. J. *Phys. Rev. B* **1994**, *50*, 13214.

MA960135I